

# Electrical and Optical Properties of Polyaniline with a Weblike Morphology

Kaushik Mallick,<sup>1</sup> Michael Witcomb,<sup>2</sup> Rudolph Erasmus,<sup>3</sup> André Strydom<sup>4</sup>

<sup>1</sup>Advanced Materials Division, Mintek, Private Bag X3015, Randburg 2125, South Africa

<sup>2</sup>Microscopy and Microanalysis Unit, University of the Witwatersrand, Private Bag 3, WITS 2050, South Africa

<sup>3</sup>School of Physics, University of the Witwatersrand, Private Bag 3, WITS 2050, South Africa

<sup>4</sup>Physics Department, University of Johannesburg, PO Box 524, Auckland Park 2006, South Africa

Received 8 July 2009; accepted 10 September 2009

DOI 10.1002/app.31441

Published online 5 January 2010 in Wiley InterScience (www.interscience.wiley.com).

**ABSTRACT:** We report on the preparation method of nanostructured polyaniline (PANI) via the oxidation polymerization of aniline hydrochloride in the presence of an anionic surfactant. Two solvents with different polarities were used for the synthesis of PANI. The polymers were characterized with ultraviolet–visible, infrared, Raman, and X-ray photoelectron spectroscopy. The chemical structure derived from the optical characterization techniques and the electrical properties for the two polymers were

almost identical. Transmission electron and scanning electron microscopy images revealed the morphological disparity between the PANIs synthesized under different solvent conditions: a microweb of nanofibers versus microtubes. © 2010 Wiley Periodicals, Inc. *J Appl Polym Sci* 116: 1587–1592, 2010

**Key words:** conducting polymers; ESCA/XPS; nanotechnology; Raman spectroscopy

## INTRODUCTION

Polyaniline (PANI) is one of the most extensively studied electroactive polymers because of its environmental stability, high degree of processability, and interesting redox properties. The ability of PANI to exist in a large number of intrinsic redox states makes it a unique and interesting class of polymeric material. PANI is a conducting polymer that has been widely studied for electronic and optical applications.<sup>1</sup> Unlike other conjugated polymers, PANI has a simple and reversible doping chemistry that enables control over properties such as solubility,<sup>2</sup> electrical conductivity,<sup>3</sup> and optical activity.<sup>4,5</sup> In recent years, one-dimensional PANI nanostructures, including nanowires, nanorods, and nanotubes, have been studied with the expectation that such materials will possess the advantages of both low-dimensional systems and organic conductors. So far, various methods have been developed for the synthesis of one-dimensional PANI nanostructures, such as the polymerization of aniline with hard templates<sup>6</sup> or in the presence of soft templates.<sup>7–14</sup>

PANI can be prepared by either chemical or electrochemical oxidative polymerization.<sup>15,16</sup> In general, one must polymerize aniline in a medium comprised of a protonic acid; the latter simultaneously also acts as a dopant to protonate as-synthesized PANI, which results in a conductive state. PANI has also been prepared directly from an aqueous medium without any protonic acid at the beginning of polymerization.<sup>17–19</sup> The morphology of the PANI obtained in such a system shows mainly either short solid or hollow nanorods, including some nonfibrous particulates.<sup>20–22</sup>

Recently, using auric acid as the oxidizing agent, we successfully synthesized one-dimensional PANI nanofibers with diameters around 50 nm without using a template<sup>23</sup> and in which aniline hydrochloride served as the precursor of PANI. In this article, we report on the synthesis of uniform-diameter, relatively long PANI nanofibers with a weblike morphology; these were produced when methanol was used as the solvent and when aniline hydrochloride served as the precursor of PANI in the presence of sodium dodecyl sulfate (SDS). We observed that the solvent played a crucial role with regard to the resulting morphology. Such a synthesis can be accomplished in a one-pot process with a wide choice of solvent and reagent concentrations.

Correspondence to: K. Mallick (kaushikm@mintek.co.za) or A. Strydom (amstrydom@uj.ac.za).

Contract grant sponsor: Project Autek (to K.M.).

Contract grant sponsor: National Research Foundation of South Africa (to A.S.); contract grant number: 2072956.

## EXPERIMENTAL

### Synthesis

All of the chemicals were analytical grade and were used as received. Typically, the polymer synthesis

reaction was performed in a 50-mL beaker. A 0.01 mol amount of aniline hydrochloride was dissolved in methanol (20 mL). Ammonium peroxydisulfate (0.01 mol) was dissolved in 10 mL of distilled water. SDS (0.002 mol) was prepared in deionized water at room temperature. A dilute solution of SDS was slowly added to the aniline hydrochloride solution under stirring. Subsequently, 0.01 mol of ammonium peroxydisulfate was added dropwise to this solution. A green precipitate formed at the bottom of the beaker. This was then allowed to settle for 1 h before filtration. The whole process was carried out at room temperature ( $\sim 25^\circ\text{C}$ ). In a separate experiment, 0.01 mol of aniline hydrochloride was dissolved in water, and the previous procedure was followed. After filtration, the solid mass from both experiments was dried *in vacuo*. A small fraction of each dried mass was deposited onto lacey, carbon coated, copper transmission electron microscopy (TEM) grids for TEM and scanning electron microscopy (SEM) analysis. The resulting material was also characterized with ultraviolet-visible (UV-vis), IR, and Raman, and X-ray photoelectron spectroscopy (XPS).

### Characterization techniques

TEM studies of the composite were carried out at an accelerating voltage of 197 kV with a Gatan GIF TriDiem on a Philips CM200 TEM equipped with an  $\text{LaB}_6$  source. SEM studies were undertaken in a FEI FEG Nova 600 Nanolab at 5 kV. For UV-vis spectral analysis, a small portion of the solid sample was dissolved in methanol and scanned within the range 300–800 nm with a Varian Cary 1E digital spectrophotometer. Raman spectra were acquired with the green (514.5 nm) line of an argon ion laser as the excitation source. Light dispersion was undertaken via the single spectrograph stage of a Jobin-Yvon T64000 Raman spectrometer. The power at the sample was kept very low (0.73 mW), whereas the laser-beam diameter at the sample was about 1  $\mu\text{m}$ . A PerkinElmer 2000 Fourier transform infrared (FTIR) spectrometer, operating within the range 850–1700  $\text{cm}^{-1}$  with a resolution 4  $\text{cm}^{-1}$ , was used for the IR spectral analyses. For this study, the sample was deposited in the form of a thin film on an NaCl disk. The XPS spectra were collected in an ultra high vacuum (UHV) chamber attached to a Physical Electronics 560 electron spectroscope for chemical analysis/scanning Auger microprobe (SAM) instrument.

For bulk electrical conductivity measurements, material was obtained in the form of high-pressure pellets. Silver paste contacts were painted directly onto the pellets. The direct-current electrical conductivity was performed under controlled temperatures with a physical properties measurement system (Quantum Design, San Diego, CA).

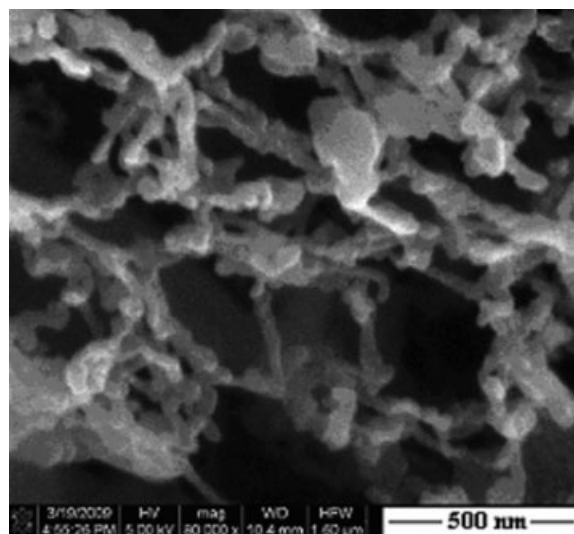


**Figure 1** SEM image of the PANI synthesized with methanol as the solvent. Synthesis conditions: [Aniline hydrochloride] = 0.01 mol, [Ammonium peroxydisulfate] = 0.01 mol, and [SDS] = 0.002 mol.

## RESULTS AND DISCUSSION

Generally, the polymerization of aniline in a concentrated solution of SDS produces a granular form of PANI,<sup>24–26</sup> whereas PANI nanofibers are obtained in high-acidic conditions.<sup>27–30</sup> It was reported that PANI rectangular microtubes were synthesized by the oxidation of aniline in a dilute SDS solution.<sup>31</sup> A low-concentration SDS and hydrochloric acid solution was recorded to create nanostructure-covered rectangular submicrotubes of PANI.<sup>32</sup>

Aniline hydrochloride was used as a precursor to avoid the addition of external protonic acid as the dopant and its resulting influence on the final morphology of the polymer product. TEM and SEM images revealed a weblike structure for the PANI, as shown in Figure 1, when PANI was synthesized in the presence of methanol. The PANI fibers, the basic unit of the web, presumably initially formed and then connected with each other to fabricate the weblike structure. The fiber diameter varied from 75 to 100 nm. When water was used as the solvent for the polymerization of aniline hydrochloride in the presence of a 0.002-mol concentration of SDS, PANI microtubes were formed, typically up to 6  $\mu\text{m}$  in length and up to 1  $\mu\text{m}$  in diameter (Fig. 2).

The electronic absorption spectrum of the PANI salt was documented previously.<sup>33</sup> The PANI salt shows three absorption peaks at 310–360, 400–440, and above 700 nm. The absorption peak at 310–360 nm is due to the  $\pi$ - $\pi^*$  transition of the benzenoid rings. The peak at 400–440 nm is due to the polaron-bipolaron transition, whereas the broad absorption band appearing above 700 nm is due to the benzenoid-to-quinoid excitonic transition. In this

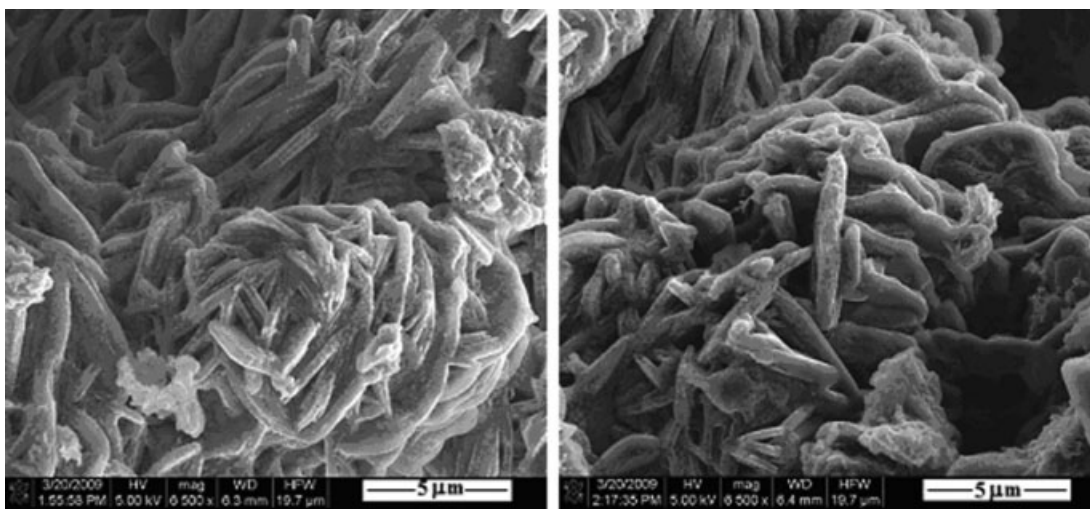


**Figure 2** SEM images of the PANI synthesized with water as the solvent. Aniline hydrochloride was used as the precursor, and ammonium peroxydisulfate was used as the oxidizing agent in the presence of SDS. Synthesis conditions: [Aniline hydrochloride] = 0.01 mol, [Ammonium peroxydisulfate] = 0.01 mol, and [SDS] = 0.002 mol.

study, the UV-vis spectrum of PANI (Fig. 3), which was synthesized with methanol as a solvent and with a weblike morphology, showed three absorption bands with peaks at 315, 435 (circled), and 760 nm, which corresponded to the aforementioned transitions. When water was used as the solvent, the UV-vis spectrum of PANI showed similar characteristic features (inset, Fig. 4) with absorption bands at 320, 430 (circled), and 720 nm. The PANI formed was either neutral or basic because the benzenoid-quinoid excitonic transition showed a broad absorption peak at 620 nm.<sup>34</sup> The shifting of the excitonic peak depends on various factors, such as the counterions, solvent, pH value, chemical structure, and morphology of the polymer.<sup>35,36</sup>

Various kinds of information are available from the principal features of typical XPS spectra.<sup>37</sup> From the characteristic binding energies of the photoelectrons, the elements involved can be identified, whereas the peak intensities can be directly related

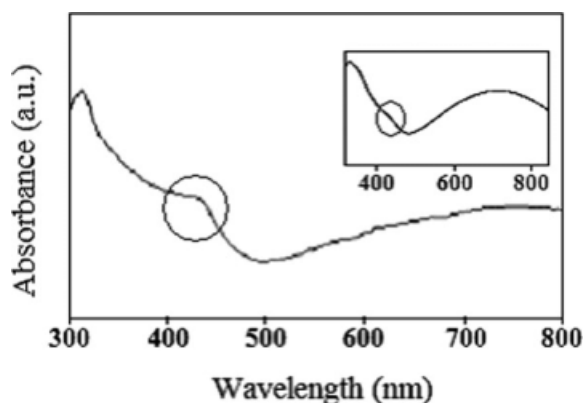


**Figure 3** UV-vis spectrum of the PANI synthesized with methanol and (in the inset) with water as the solvent. The peaks around 430 nm are circled for clarity.

to the atomic concentration of the elements in the sample. In this case, the most important features of XPS were its ability to measure shifts in the binding energy of the core-level electrons, which result from changes in their chemical environment, and the quantitative analysis of the various intrinsic redox

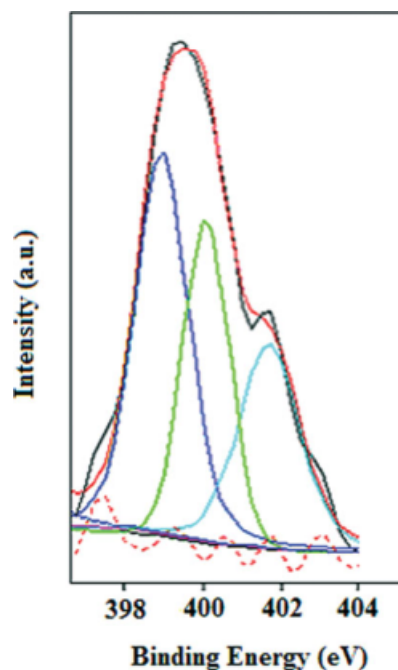


**Figure 4** XPS spectra of the PANI synthesized with methanol as a solvent differentiated by the curve fitting of the N1s core-level spectrum. Deconvolution of the spectrum yielded three distinct curves, which were related to the quinoid imine (peak center at 398.14 eV), benzenoid amine (peak center at 399.85 eV), and positively charged nitrogen (peak center at 401.21 eV). [Color figure can be viewed in the online issue, which is available at [www.interscience.wiley.com](http://www.interscience.wiley.com).]

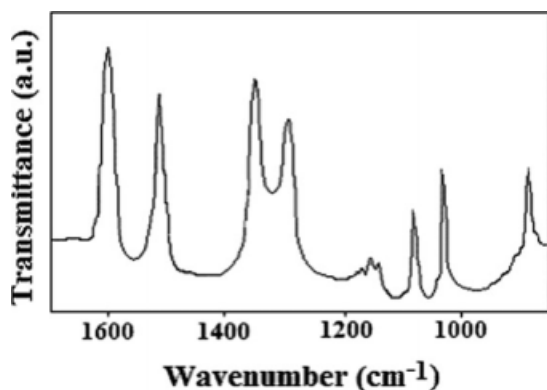


**Figure 5** FTIR spectrum for the PANI sample (synthesis conditions: [Aniline hydrochloride] = 0.01 mol, [Ammonium peroxydisulfate] = 0.01 mol, [SDS] = 0.002 mol, and solvent = methanol) within the spectral region from 1700 to 850  $\text{cm}^{-1}$ . The peak at 1600  $\text{cm}^{-1}$  corresponded to the group  $\text{N}=\text{Q}=\text{N}$ , whereas the  $\text{N}-\text{B}-\text{N}$  group was represented by the peak at 1520  $\text{cm}^{-1}$ .

states of PANI. Usually, the XPS spectra of the N1s core line of the PANI can be deconvoluted into three environments, namely, quinoid imine ( $-\text{N}=\text{}$ ), benzenoid amine ( $-\text{NH}-$ ), and positively charged nitrogen ( $-\text{NH}^+$ ), depending on the protonation states, and these can be differentiated by the curve fitting of the N1s core-level spectrum; the environments were observed at below 399, 399–400, and above 400 eV, respectively.<sup>38,39</sup> For the PANI sample synthesized with methanol as the solvent, the XPS spectra (Fig. 5) could also be deconvoluted into three distinct curves, which were related to the quinoid imine (peak center at 398.88 eV), benzenoid amine (peak center at 399.86 eV), and positively charged nitrogen (peak center at 401.63 eV). Table I lists the peak positions derived from the XPS N1s spectral analysis of the two PANI samples synthesized with the two different solvents. When PANI was synthesized with dodecylbenzene sulfonic acid, two  $\text{N}^+$  species were observed in the XPS spectra above 400 eV.<sup>40</sup> These two  $\text{N}^+$  species were attributed to different protonation environments and the formation of polaron and bipolaron species at lower and higher electronvolts, respectively. These indicated the excess protonation of the PANI.<sup>40</sup> Because no excess protonic acid was added as a dopant in this experiment, the only available source of protonic acid was the aniline hydrochloride precursor.

From the UV–vis and the XPS spectral analysis, we confirmed that the chemical structure of the two kinds of PANI we produced were similar in nature. In addition to this investigation, we also examined the spectroscopic behavior of the resulting materials by FTIR spectral analysis within the spectral region from 1700 to 850  $\text{cm}^{-1}$  (Fig. 5). IR analysis of this fingerprint region was particularly useful for examination of the resonance modes of the benzenoid and

**TABLE I**  
Peak Positions Derived from XPS N1s Spectral Analysis of the Two PANI Samples Synthesized with Methanol and Water as the Solvents

Sample	Species	Peak center (eV)
PANI with methanol solvent	$-\text{N}=\text{}$	394.88
	$-\text{NH}-$	399.86
	$\text{NH}^+$	401.63
PANI with water solvent	$-\text{N}=\text{}$	398.25
	$-\text{NH}-$	399.56
	$\text{NH}^+$	402.02

quinoid units and the individual bonds of the compound. In the IR spectra, the peak at 1600  $\text{cm}^{-1}$  corresponded to the  $\text{N}=\text{Q}=\text{N}$  group (where Q represents a quinoid ring), whereas the  $\text{N}-\text{B}-\text{N}$  group (where B represents a benzenoid ring) absorbed at 1520  $\text{cm}^{-1}$ . The band at 1365  $\text{cm}^{-1}$  was attributed to the C–N stretching mode in the neighborhood of the quinoid ring. The band at 1300  $\text{cm}^{-1}$  was assigned to the C–N stretching of the aromatic amine, whereas in the region 1160–1040  $\text{cm}^{-1}$ , the aromatic in-plane C–H bending modes were seen. Spectroscopic analysis confirmed that the aniline oxidation product obtained in acid media had a predominantly head-to-tail ( $-\text{N}-\text{Ph}-\text{N}-\text{Ph}-$ ) arrangement, where Ph is the benzene ring.<sup>41</sup> The out-of-plane deformation of C–H in the 1,4-disubstituted benzene ring was located at 860  $\text{cm}^{-1}$ .

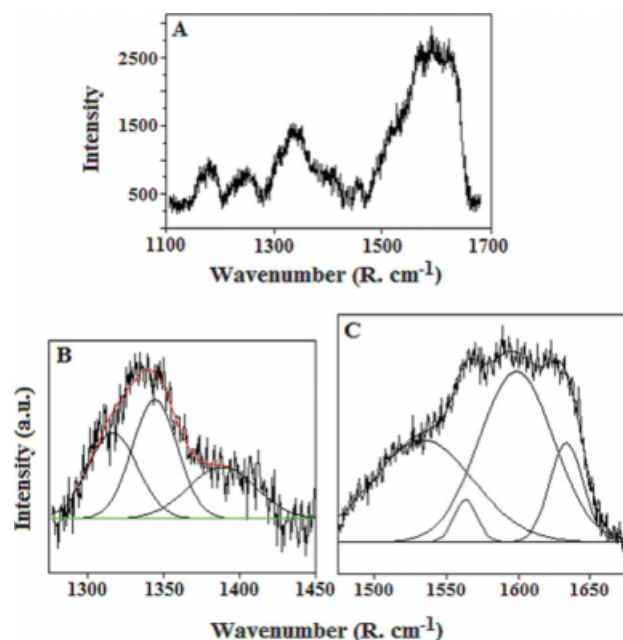


**Figure 6** Raman spectra of the PANI synthesized in the presence of methanol as the solvent: (A) overall spectrum covering the range from 1100 to 1700  $\text{cm}^{-1}$  and (B,C) expanded and deconvoluted spectra from the 1250–1450 and 1450–1700- $\text{cm}^{-1}$  regions, respectively. [Color figure can be viewed in the online issue, which is available at [www.interscience.wiley.com](http://www.interscience.wiley.com).]

Figure 6 shows a typical Raman spectrum recorded for PANI. In this spectrum obtained from our synthesized material, the bands between 1100 and 1700  $\text{cm}^{-1}$  [Fig. 6(A)] were sensitive to the PANI oxidation state. Figure 6(B,C) shows the expanded regions 1250–1450 and 1450–1700  $\text{cm}^{-1}$ , respectively, of Figure 6(A) and shows the deconvoluted spectrum from each. The spectrum of the PANI nanoweb obtained in the presence of an anionic micelle revealed C–C deformation bands of the benzoid ring at 1630 and 1595  $\text{cm}^{-1}$ , which are characteristic of semiquinone rings.<sup>42,43</sup> The band at 1530  $\text{cm}^{-1}$  corresponded to the N–H bending deformation band of protonated amine. Intense overlapping features between 1300 and 1425  $\text{cm}^{-1}$  with peak positions at 1320, 1345, and 1390  $\text{cm}^{-1}$  corresponded to the C–N<sup>•+</sup> stretching modes of delocalized polaronic charge carriers and confirmed the high concentration of these forms present in the PANI sample. The broad band at 1245  $\text{cm}^{-1}$  was assigned to the C–N stretching mode of the polaronic units. The position of the benzene C–H bending deformation band at 1171  $\text{cm}^{-1}$  was characteristic of the reduced and semiquinone structures in the polymer sample. A typical Raman spectrum of the PANI obtained from the aniline hydrochloride precursor included a band at 1470  $\text{cm}^{-1}$ , which corresponded to the C=N stretching mode of the quinoid units. The presence of another two bands at 1245 and 1470  $\text{cm}^{-1}$  indicated that there were a lot of separated, and thus localized, single and double bonds available in the PANI structure. The positions of the C–C and C–H benzene deformation modes fell at 1630, 1595, and 1171  $\text{cm}^{-1}$ , respectively; this indicated the presence of quinoid rings in the polymer backbone.

TEM and SEM images provided evidence of the directional growth of the polymer. The mechanism for this directional growth could be understood by reference to classical nucleation theory. The accepted mechanism is of a two-step process, such as the formation of the nucleation centers followed by their successive growth. In the first step, we can assume that, initially, the oligomeric form of PANI occurred because of the presence of a suitable oxidizing agent. The oligomer may have acted as a nucleation center, which catalyzed the oxidation of the remaining monomers present in the solution. The formation of a branched network when PANI formed the weblike morphology can be explained as follows. A competition between the directional growth process of the polymer and the formation of additional nucleation centers took place. Once a high density of nucleation centers was generated, the interfacial energy between the reaction solution and the polymer may have been minimized, and hence, rapid precipitation occurred in a disordered manner;<sup>14,44</sup> this yielded irregular shapes, such as the weblike morphology observed here.

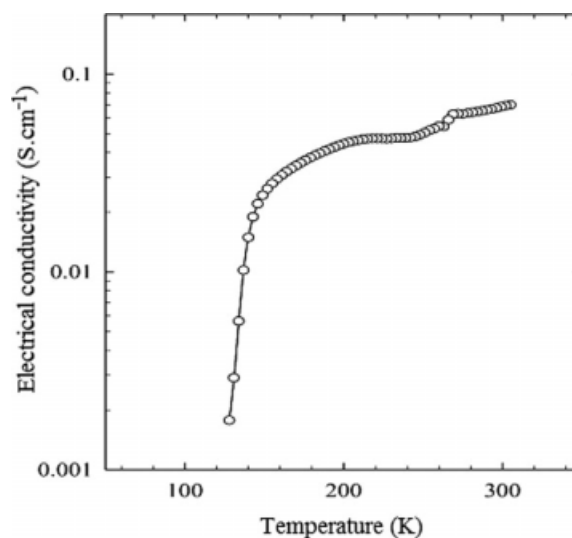


**Figure 7** Semilog plot of the temperature dependence of the electrical conductivity of the PANI prepared with methanol as the solvent.

Figure 7 shows the temperature ( $T$ ) dependence of the electrical conductivity of the methanol-solvent-prepared sample of PANI on a semilog scale. Near and below room temperature, the conductivity ( $\sigma$ ) amounted to  $\sigma \approx 0.1 \text{ S/cm}$ , which was many orders of magnitude over that of typical polymer materials. We observed only a weak temperature dependence,  $\sigma \propto T$ , of the conductivity of our weblike material, but, interestingly, the conductivity was found to increase with temperature. We note in this regard the work of Kulikov et al.<sup>45</sup> who used an electron spin resonance study to support the concept that electrical conductivity is severely impeded by polaron motion within amorphous regions of a material, compared to crystalline regions, and by the low mobility of polarons in boundary regions between amorphous regions. We propose that the observed increase in conductivity near room temperature may be explained by the decay of optical phonon modes that acted as an effective scattering mechanism for polaron conduction. The decay was likely into low-energy phonons that did not couple with polarons. The existence of optical phonons in this material should have been expected because the material was largely amorphous and, thus, of low overall crystallinity. We note that the opposite case prevails in crystalline materials and metals, where the abundance of acoustic phonon modes near room temperature rather cause a decrease in the conductivity according to  $\sigma^{-1} \propto \rho \propto T$  because of the increasing scattering of electrons that are primarily responsible for charge conduction in metals.

Solvent-based protonation-induced electrical conduction of PANI is well known,<sup>46</sup> and reports of solid-state PANI protonation by camphorsulfonic

acid<sup>47</sup> have broadened the method even further. The doping concentration dependence of conductivity<sup>48</sup> has demonstrated that control of the conductivity may be an important attribute of electrical materials engineered in this way.

## CONCLUSIONS

In this study, we demonstrated a facile synthesis route of PANI with different morphology using ammonium peroxydisulfate as an oxidizing agent in the presence of an anionic surfactant using two different kinds of solvents. From the UV-vis, XPS, FTIR, and Raman spectral analysis, we confirmed that the chemical structure of the two kinds of PANI produced were similar in nature. Electrical conductivity results show this approach for the preparation of PANI to be equally amenable to engineering an electrical conducting material. We believe that the positive temperature coefficient of conductivity (conductivity increasing with temperature) found in this study near room temperature warrants further investigations, as this might point the way forward for the control and novel ways of enhancing the electrical conductivity in this and related materials.

One author (A.S.) acknowledges financial aid from the University of Johannesburg Research Committee and the Faculty of Science.

## References

1. Skotheim, T. A.; Elsenbaumer, R. L.; Reynolds, J. R. *Handbook of Conducting Polymers*; Marcel Dekker: New York, 1997.
2. Cao, Y.; Smith, P.; Heeger, A. J. *Synth Met* 1993, 57, 3514.
3. Chiang, J. C.; MacDiarmid, A. G. *Synth Met* 1986, 13, 193.
4. Xia, Y. N.; Wiesinger, J. M.; MacDiarmid, A. G.; Epstein, A. J. *Chem Mater* 1995, 7, 443.
5. Majidi, M. R.; KaneMaguire, L. A. P.; Wallace, G. G. *Polymer* 1994, 35, 3113.
6. Wu, C. G.; Bein, T. *Science* 1994, 264, 1757.
7. Zhang, Z.; Wei, Z.; Wan, M. *Macromolecules* 2002, 35, 5937.
8. Carswell, A. D. W.; O'Rear, E. A.; Grady, B. P. *J Am Chem Soc* 2003, 125, 14793.
9. Huang, L.; Wang, Z.; Wang, H.; Cheng, X.; Mitra, A.; Yan, Y. *J Mater Chem* 2002, 12, 388.
10. Zhang, X.; Goux, W. J.; Manohar, S. K. *J Am Chem Soc* 2004, 126, 4502.
11. Marie, E.; Rothe, R.; Antonietti, M.; Landfester, K. *Macromolecules* 2003, 36, 3967.
12. Huang, J.; Kaner, R. B. *Angew Chem Int Ed* 2004, 43, 5817.
13. Huang, J.; Virji, S.; Weiller, B. H.; Kaner, R. B. *J Am Chem Soc* 2003, 125, 314.
14. Chiou, N. R.; Epstein, A. J. *Adv Mater* 2005, 17, 1679.
15. Huang, W. S.; Humphrey, B. D.; MacDiarmid, A. G. *J Chem Soc Faraday Trans* 1986, 82, 2385.
16. MacDiarmid, A. G.; Epstein, A. J. *Faraday Discuss Chem Soc* 1989, 88, 317.
17. Gospodinova, N.; Mokreva, P.; Terlemezyan, L. *Polymer* 1993, 34, 2438.
18. Palaniappan, S. *Polym Adv Technol* 2002, 13, 54.
19. Palaniappan, S.; Nivasu, V. *New J Chem* 2002, 26, 1490.
20. Konyushenko, E. N.; Stejskal, J.; Sedenkova, I.; Trchova, M.; Sapurina, I.; Cieslar, M.; Prokes, J. *Polym Int* 2006, 55, 31.
21. Trchova, M.; Sedenkova, I.; Konyushenko, E. N.; Stejskal, J.; Holler, P.; Ciric-Marjanovic, G. *J Phys Chem B* 2006, 110, 9461.
22. Stejskal, J.; Sapurina, I.; Trchova, M.; Konyushenko, E. N.; Holler, P. *Polymer* 2006, 47, 8253.
23. Mallick, K.; Witcomb, M. J.; Scurrell, M. S.; Strydom, A. M. *2008 Gold Bull* 2008, 41, 246.
24. Kim, B. J.; Im, S. S.; Oh, S. G. *Langmuir* 2001, 16, 5841.
25. Kim, B. J.; Im, S. S.; Oh, S. G. *Langmuir* 2001, 17, 565.
26. Du, J.; Zhang, J.; Han, B.; Liu, Z.; Wan, M. *Synth Met* 2005, 155, 523.
27. Huang, J.; Virji, S.; Weiller, B. H.; Kaner, R. B. *J Am Chem Soc* 2003, 125, 314.
28. Huang, J.; Kaner, R. B. *J Am Chem Soc* 2004, 126, 851.
29. Jing, X.; Wang, Y.; Wu, D.; She, L.; Guo, Y. *J Polym Sci Part A: Polym Chem* 2006, 44, 1014.
30. Khalil, H.; Levon, K. *Macromolecules* 2002, 35, 8180.
31. Zhou, C.; Han, J.; Guo, R. *J Phys Chem B* 2008, 112, 5014.
32. Zhou, C.; Han, J.; Guo, R. *Macromolecules* 2009, 42, 1252.
33. Pillalamarri, S. K.; Blum, F. D.; Tokuhira, A. T.; Bertino, M. F. *Chem Mater* 2005, 17, 5941.
34. Trivedi, D. C. *Handbook of Organic Conductive Molecules and Polymers*; Nalwa, H. S., Ed.; Wiley: New York, 1997; Vol. 2, p 529.
35. MacDiarmid, A. G.; Epstein, A. J. *Synth Met* 1995, 69, 85.
36. Min, Y.; Xia, Y.; MacDiarmid, A. G.; Epstein, A. J. *Synth Met* 1995, 69, 159.
37. Siegbahn, K.; Nordling, C.; Fahlman, A.; Nordberg, R.; Hamrin, K.; Hodman, J.; Johansson, G.; Bergmark, T.; Karlsson, S.; Lindgren, I.; Linderg, B. *ESCA: Atoms, Molecules and Solid State Structure Studies by Means of Electron Spectroscopy*; Almqvist and Wiksells: Uppsala, Sweden, 1967.
38. Li, Z. F.; Kang, E. T.; Neoh, K. G.; Tan, K. L. *Synth Met* 1997, 87, 45.
39. Li, Z. F.; Neoh, K. G.; Pun, M. Y.; Kang, E. T.; Tan, K. L. *Synth Met* 1995, 73, 209.
40. Han, M. G.; Cho, S. K.; Oh, S. G.; Im, S. S. *Synth Met* 2002, 126, 53.
41. Kang, E. T.; Neoh, K. G.; Tan, K. L. *Prog Polym Sci* 1998, 23, 277.
42. Lapkowski, M.; Berrada, K.; Quillard, S.; Louarn, G.; Lefrant, S.; Proń, A. *Macromolecules* 1995, 28, 1233.
43. Louarn, G.; Lapkowski, M.; Quillard, S.; A. Proń, A.; Buisson, J. P.; Lefrant, S. *J Phys Chem* 1996, 100, 6998.
44. Walton, A. G. *The Formation and Properties of Precipitates*; Interscience: New York, 1967.
45. Kulikov, A. V.; Bogatyrenko, V. R.; Belonogova, O. V.; Fokeeva, L. S.; Lebedev, A.; Echmaeva, T. A.; Shunina, I. G. *Russ Chem Bull* 2002, 51, 2216.
46. Stejskal, J.; Gilbert, R. G. *Pure Appl Chem* 2002, 74, 857.
47. Stejskal, J.; Sapurina, I.; Trchová, M.; Prokeš, J.; Křivka, I.; Tobolovká, E. *Macromolecules* 1998, 31, 2218.
48. Xing, S.; Zhao, C.; Jing, S.; Wang, Z. *Polymer* 2006, 47, 2305.